World Academy of Science, Engineering and Technology
International Journal of Computer and Information Engineering
Vol:11, No:7, 2017

Markov Random Field-Based Segmentation Algorithm for Detection of Land Cover Changes Using Uninhabited Aerial Vehicle Synthetic Aperture Radar Polarimetric Images

Mehrnoosh Omati, Mahmod Reza Sahebi

***Abstract*—**The information on land use/land cover changing plays an essential role for environmental assessment, planning and management in regional development. Remotely sensed imagery is widely used for providing information in many change detection applications. Polarimetric Synthetic aperture radar (PolSAR) image, with the discrimination capability between different scattering mechanisms, is a powerful tool for environmental monitoring applications. This paper proposes a new boundary-based segmentation algorithm as a fundamental step for land cover change detection. In this method, first, two PolSAR images are segmented using integration of marker-controlled watershed algorithm and coupled Markov random field (MRF). Then, object-based classification is performed to determine changed/no changed image objects. Compared with pixel-based support vector machine (SVM) classifier, this novel segmentation algorithm significantly reduces the speckle effect in PolSAR images and improves the accuracy of binary classification in object-based level. The experimental results on Uninhabited Aerial Vehicle Synthetic Aperture Radar (UAVSAR) polarimetric images show a 3% and 6% improvement in overall accuracy and kappa coefficient, respectively. Also, the proposed method can correctly distinguish homogeneous image parcels.

***Keywords*—**Coupled Markov random field, environment, object-based analysis, Polarimetric SAR images.

I. Introduction

DETECTION of land cover changes is one of the most important applications of remotely sensed data. Despite the numerous studies devoted to multispectral and hyperspectral imagery, however, the use of optical imaging sensors is limited to weather conditions [1]-[3]. Synthetic aperture radar (SAR) sensors can obtain daylight, cloud coverage, and weather-independent images [4]. Their backscattered signals are also sensitive to the form, orientation, homogeneity, and surface conditions of the different targets [5]. In recent decades, the development of PolSAR techniques with measurement of four linear polarization channels (i.e., HH, HV, VH, and VV) and the phase differences among them can serve as a useful tool for detecting land cover and land use changes [1], [6].

From the perspective of image analysis unit, Change detection techniques are classified into two categories, namely, pixel- and object-based approaches [7]. Pixel-based methods are done without consideration of the spatial relationship among pixels.

Discrete random field models, such as the MRF, are efficient way for representing the dependence between pixels in the spatial domain [8], [9]. A number of studies have been performed with the aim of improving change detection procedure using MRF models [10], [11]. In this approach, a changed image is first determined by applying a pixel-based algorithm. Then, Change detection performance is improved with the fusion spatial-contextual information on the basis of MRF models. However, this two-part algorithm presents two disadvantages [12]. First, some image information is lost as pixel-based methods are used to obtain initial change and no-change image. Second, for many transformations, MRF properties may not be preserved. To overcome these problems, different levels of image processing can perform the direct MRF-based modeling of the spatial correlation between the pixels of an observed image [12].

Various edge-based segmentation techniques have been developed for SAR and PolSAR images [13]-[16]. Classical boundary detection operators are inefficient for SAR images because of the multiplicative nature of speckle [17]. These operators thus yield poor results on edges between different regions [13].

The objective of this paper is the improvement of segmentation analysis as an initial step in object-based change detection method. The proposed boundary-based coupled MRF segmentation algorithm using spatial-contextual information enables the reduction of speckle effect in PolSAR images and improves the weak edges between different image parcels. Then, the subspace of ratio of polarimetric features is applied to detect land cover changes on the object level.

II. Theory

A. Markov Random Field

The MRF, as a branch of the probability theory, considers the spatial-contextual information for a variety of fields of image processing such as image restoration, texture analysis, edge detection, image segmentation and classification, data fusion, object matching and recognition [9]. In explanation of the theory of this statistical model [9], $F = \{F_1,...,F_m\}$ is

Mehrnoosh Omati and Mahmod Reza Sahebi are with the Faculty of Geodesy and Geomatics Engineering, K .N. Toosi University of Technology, Tehran 19697-64499, Iran (e-mail: momati@mail.kntu.ac.ir; Sahebi@kntu.ac.ir).

considered a collection of random variables that are defined on set S with m members such that each of the F_i values has a value f_i in the set of user-defined labels.

To reduce the mathematical complexity of the joint probability of MRF models, the joint probability of an MRF can be represented in the form of the Gibbs distribution [9]. Therefore, the joint distribution of an MRF takes the following form [9]:

$$P(f) = \frac{1}{Z}\exp\left[\frac{-U(f)}{T}\right]$$

$$Z = \sum_{allpossibl\ econfigura\ tionsoff} \exp\left[\frac{-U(f)}{T}\right] \quad (1)$$

where T is a constant denominated temperature, $U(f)$ is called energy function, and Z is a normalizing constant (the partition function).

According to the equation above, the maximization of $P(f)$ is equivalent to the minimization of the energy function.

B. Coupled MRF Model

In this proposed model, the input image is considered as a coupled MRF pair (x, l) where x is the $M \times N$ lattice for the intensity field, and l is the dual lattice for line field [11]. In the MRF model, a lattice of m pixel sites and the dual lattice for edge field are represented respectively by following notations [9]:

$$S^P = \{i | 1 \le i \le m\} \quad (2)$$

$$S^E = \{(i,i') | i \in S^P, i' \in S^P, i' \in N_i\} \quad (3)$$

where i and i' are neighbors and N_i is the neighborhood system.

The integration between these coupled MRFs using the prior energy $U(f^P, f^E)$ can be expressed as:

$$U(f^P, f^E) = \sum_{i \in S^P} \sum_{i' \in N_i} g(f_i^P, f_{i'}^P, f_{i,i'}^E)$$

$$= \sum_{i \in S^P} \sum_{i' \in N_i} [(f_i^P - f_{i'}^P)^2 (1 - f_{i,i'}^E) + \alpha f_{i,i'}^E \quad (4)$$

where $g(.,.,.)$, is clique potential function, f_i^P is an intensity label with a value in a real interval L^P, $f_{i'}^P$ is neighboring intensity label, $f_{i,i'}^E$ is an edge label with a value in $L^E = \{0,1\}$, and cost of α is a parameter associated with controlling the exceeding number of discontinuities of intensity values between neighboring areas.

With the adding the prior energy and the likelihood energy, the posterior energy can be determined by following equation:

$$U(f^P, f^E \mid d) = \sum_{i \in S^P} (f_i^P - d_i)^2 + \sum_{i \in S^P} \sum_{i' \in N_i} \lambda g(f_i^P, f_{i'}^P, f_{i,i'}^E) \quad (5)$$

where d_i is the observed data, and λ is called the smoothing parameter. Posterior energy in (5) can be converted to (6) with a simpler form, as rewritten below:

$$U(f^P, f^E \mid d) = \sum_{i \in S^P} (f_i^P - d_i)^2 + \sum_{i \in S^P} \sum_{i' \in N_i} \lambda g'(f_i^P - f_{i'}^P) \quad (6)$$

where

$$g'(f_i^P - f_{i'}^P) = \min\{(f_i^P - f_{i'}^P)^2, \alpha\} \quad (7)$$

Iterative minimization of this equation with respect to only f^P leads to the restored image $(f^P)^*$, in which its values of pixels near discontinuities are well preserved. Then by the thresholding of $(f^P)^*$, the edge field is determined as follows:

$$f_{i,i'}^E = \begin{cases} 1 & \text{if } (f_i^P - f_{i'}^P)^2 > \alpha \\ 0 & \text{otherwise} \end{cases} \quad (8)$$

III. Study Area and Data Set

The study area of this work was selected near to Sacramento-Joaquin Delta in southern California, USA. The localization of this area is shown in Fig. 1. The land cover of test area consists of agriculture, water, bare land, urban areas. Two UAVSAR L-band full polarimetric images are acquired on 18 July 2009 and 14 August 2014. The data is obtained with a spatial resolution of 1.8 m in the range and 0.8 m in azimuth direction, and incidence angle range from 25 degrees to 65 degrees. The subset images are selected over the agricultural lands as the area of interest.

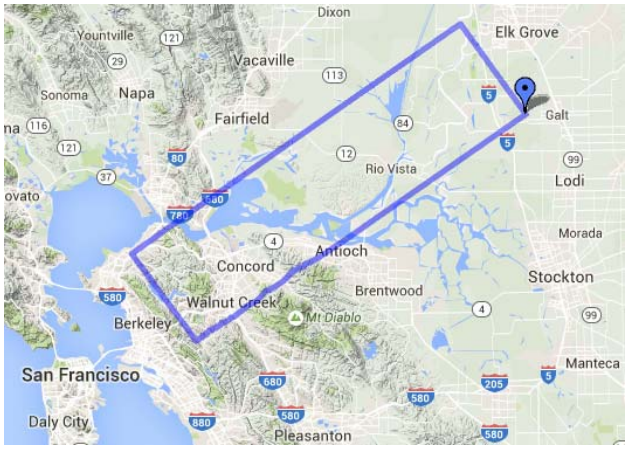

Fig. 1 Study area

IV. Results and Discussion

A. Preprocessing of PolSAR Images

As one of the major steps in change detection for PolSAR images, preprocessing involves radiometric calibration, image co-registration, and speckle filtering. With the conversion of intensity values to backscattering coefficients in radiometric

calibration, each pixel of SAR image directly represents the portion of microwave backscatter from a scene. Filtering technique is performed to reduce the speckle effect while also minimization information loss enables the better discrimination of scene targets. In this study, the Frost filter with a windows size of 5×5 and a damping factor of 2 is used as the best filter. In another pre-processing step, precise image co-registration is performed in Nest 5.1, wherein 200 ground control points in images are automatically selected. These points are evenly distributed throughout the images, after which two georeferenced polarimetric images are registered with each other at an accuracy of 0.5 pixels.

B. Results of Coupled MRF for Edge Detection

The boundary-based coupled MRF algorithm was employed to segment a single image resulting from the sum of the squares of the diagonal elements in the covariance matrix (span image). We evaluated the effects of the values of penalty parameter in the coupled MRF model by using the overall error percentage, false positive (FP), and false negative (FN) as criteria. The overall error percentage is given by (9),

$$\left(\frac{FN+FP}{TP+TN+FP+FN}\right)\times 100 \tag{9}$$

where TP, TN, FP, and FN are defined as:

- TP: the number of pixels that correctly detected as the edge.
- TN: the number of pixels that correctly detected as the no-edge.
- FP: the number of pixels that incorrectly detected as the edge.
- FN: the number of pixels that incorrectly detected as the no- edge.

With increasing parameter value, two overall error percentages and FP significantly decrease, whereas the FN gradually increases. As the threshold value for the proposed edge detection algorithm, an increasing penalty parameter enables the detection of fewer extra edges and disregards more reference edge pixels. Thus, with balance among the overall error percentage, FP, and FN, the values of α are set to 500 and 300 for the images taken on 18 July 2009 and 21 August 2014, respectively.

In this study, the proposed edge detection algorithm, Canny and Laplacian of Gaussian (LoG) edge detectors are visually compared for each of the PolSAR images. For the image acquired on 18 July 2009, the high threshold and standard deviation of the Gaussian filter of canny edge detector are fixed to 0.3 and 1, respectively. In the LoG edge detection operator, the threshold and standard deviation of the LoG filter are set to 30 and 1, respectively. For the image acquired on 21 August 2014, a high threshold value of 0.2 and a Gaussian filter standard deviation of 1 are good values for detecting edges through the canny edge detector. The LoG edge detector has values of 20 and 1 for the threshold and standard deviation of the LoG filter. Figs. 2 and 3 show the visual results of the three methods used in the detection of edges in two images.

C. Integrating the Results of the Region-Based Watershed and Coupled MRF Algorithm

Fig. 4 presents the results of the integration of coupled MRF-based edge extraction and region-based marker-controlled watershed for two PolSAR images. The findings indicate that the weak, missing, and discontinuous edges are significantly improved with the use of additional edge information and homogeneous agricultural image objects are distinguished correctly.

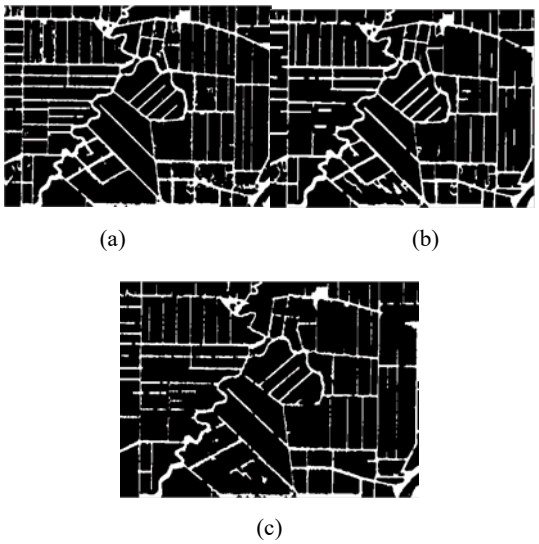

Fig. 2 Implementation of edge detection methods on 18 July 2009, (a) proposed coupled MRF method, (b) Canny edge detector, (c) LoG edge detector

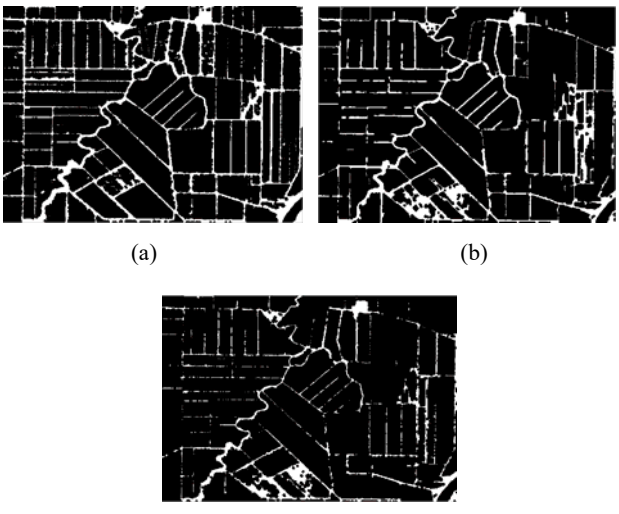

Fig. 3 Implementation of edge detection methods on 21 August 2014, (a) proposed coupled MRF method, (b) Canny edge detector, (c) LoG edge detector

D. Change Detection Results

In this work, pixel and object-based binary classification is performed using an SVM classifier for the subspace of ratios of polarimetric features. In the object-based approach, for the

subset of polarimetric features, the mean values of pixels are calculated for each homogeneous image object obtained from the proposed segmentation method. Then, to perform object-based classification, SVM is used with the ratios of the mean values of selected features in the corresponding image objects of two images. The confusion matrix of binary classification for pixel and object-based approach is provided in Tables I and II. The results show that using spatial information in object-based analysis can significantly reduce speckle effects in PolSAR images and effectively improve classification results. Fig. 5 shows the results of binary pixel and object-based classification.

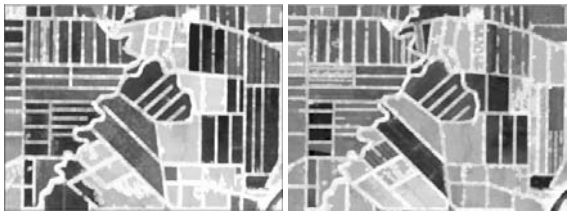

(a) (b)

Fig. 4 Integration of the edge and region-based segmentation algorithms: (a) 18 July 2009 image, (b) 21 August 2014 image

TABLE I
THE CONFUSION MATRIX OF BINARY CLASSIFICATION IN OBJECT-BASED APPROACH

		True Class		
	Classes	Changed	Unchanged	User accuracy
Classified image	Changed	369	0	100%
	Unchanged	96	509	84.13%
	Producer accuracy	79.35%	100%	
		Overall accuracy: 90.14%		
		Kappa coefficient: 0.8		

TABLE II
THE CONFUSION MATRIX OF BINARY CLASSIFICATION IN PIXEL -BASED APPROACH

		True Class		
	Classes	Changed	Unchanged	User accuracy
Classified image	Changed	373	30	92.56%
	Unchanged	92	479	83.89%
	Producer accuracy	80.22%	94.11%	
		Overall accuracy: 87.47%		
		Kappa coefficient: 0.74		

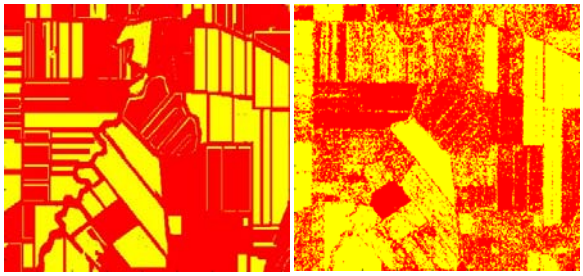

Fig. 5 the results of change detection (a) object-based method, (b) pixel-based method

V. CONCLUSION

In this paper, we have presented a novel boundary-based segmentation algorithm for change detection of agricultural land cover. Two UAVSAR polarimetric images acquired on 18 July 2009 and 21 August 2014 are used. The proposed method first involves the segmentation of two PolSAR images through the integrating of the region-based watershed algorithm and the edge-based coupled MRF. Then, an SVM classifier is used to carry out object-based classification based on the ratios of the mean values of the subset of polarimetric features in corresponding image objects. This object-based change detection approach reduces the speckle effect in the PolSAR images and improves the results of pixel-based classification. Also, the coupled MRF edge detection that considers spatial information improves the weak boundaries between image objects and enables accurate segmentation as a fundamental step in the proposed object-based change detection method.

ACKNOWLEDGMENT

The authors would like to thank American JPL/NASA, for providing the data set, and the remote sensing research center of K.N Toosi University of technology.

REFERENCES

[1] Z. Qi, A. G.-O. Yeh, X. Li, and X. Zhang, "A three-component method for timely detection of land cover changes using polarimetric SAR images," *ISPRS Journal of Photogrammetry and Remote Sensing*, vol. 107, pp. 3-21, 2015.

[2] A. N. French, T. J. Schmugge, J. C. Ritchie, A. Hsu, F. Jacob, and K. Ogawa, "Detecting land cover change at the Jornada Experimental Range, New Mexico with ASTER emissivities," *Remote Sensing of Environment,* vol. 112, pp. 1730-1748, 2008.

[3] M. A. Friedl, D. Sulla-Menashe, B. Tan, A. Schneider, N. Ramankutty, A. Sibley, et al., "MODIS Collection 5 global land cover: Algorithm refinements and characterization of new datasets," *Remote Sensing of Environment,* vol. 114, pp. 168-182, 2010.

[4] G. Moser and S. B. Serpico, "Generalized minimum-error thresholding for unsupervised change detection from SAR amplitude imagery," *IEEE Transactions on Geoscience and Remote Sensing*, vol. 44, pp. 2972-2982, 2006.

[5] A. A. Nielsen, H. Skriver, and K. Conradsen, "Complex Wishart Distribution Based Analysis of Polarimetric Synthetic Aperture Radar Data," *in International Workshop on the Analysis of Multi-temporal Remote Sensing Images*, 2007, pp. 1-6.

[6] M. Salehi, M. R. Sahebi, and Y. Maghsoudi, "Improving the accuracy of urban land cover classification using Radarsat-2 PolSAR data," *IEEE Journal of Selected Topics in Applied Earth Observations and Remote Sensing*, vol. 7, pp. 1394-1401, 2014.

[7] M. Hussain, D. Chen, A. Cheng, H. Wei, and D. Stanley, "Change detection from remotely sensed images: From pixel-based to object-based approaches," *ISPRS Journal of Photogrammetry and Remote Sensing,* vol. 80, pp. 91-106, 2013.

[8] F. Baselice, G. Ferraioli, and V. Pascazio, "Markovian change detection of urban areas using very high resolution complex SAR images," *IEEE Geoscience and Remote Sensing Letters*, vol. 11, pp. 995-999, 2014.

[9] S. Z. Li, *Markov random field modeling in image analysis*: Springer Science & Business Media, 2009, pp.1–3.

[10] S.-E. Park, Y. Yamaguchi, and D.-j. Kim, "Polarimetric SAR remote sensing of the 2011 Tohoku earthquake using ALOS/PALSAR," *Remote Sensing of Environment,* vol. 132, pp. 212-220, 2013.

[11] Y. Chen and Z. Cao, "An improved MRF-based change detection approach for multitemporal remote sensing imagery," *Signal processing*, vol. 93, pp. 163-175, 2013.

[12] T. Kasetkasem and P. K. Varshney, "An image change detection algorithm based on Markov random field models," *IEEE Transactions*

on Geoscience and Remote Sensing, vol. 40, pp. 1815-1823, 2002.
[13] R. Fjørtoft, A. Lopes, P. Marthon, and E. Cubero-Castan, "An optimal multiedge detector for SAR image segmentation, " *IEEE Transactions on Geoscience and Remote Sensing,* vol. 36, pp. 793-802, 1998.
[14] R. Touzi, A. Lopes, and P. Bousquet, "A statistical and geometrical edge detector for SAR images," *IEEE Transactions on geoscience and remote sensing*, vol. 26, pp. 764-773, 1988.
[15] C. Oliver and P. Lombardo, "Simultaneous mean and texture edge detection in SAR clutter," *IEE Proceedings-Radar, Sonar and Navigation*, vol. 143, pp. 391-399, 1996.
[16] J. Schou, H. Skriver, A. A. Nielsen, and K. Conradsen, "CFAR edge detector for polarimetric SAR images, "*IEEE Transactions on Geoscience and Remote Sensing,* vol. 41, pp. 20-32, 2003.
[17] G. Ferraioli, "Multichannel InSAR building edge detection," *IEEE Transactions on Geoscience and Remote Sensing*, vol. 48, pp. 1224-1231, 2010.

Mehrnoosh Omati received the M.Sc. degree in Geomatics engineering from K.N Toosi University of Technology, Tehran, Iran, in 2016. She is currently working toward the Ph.D. degree in remote sensing at K.N Toosi University of Technology, Tehran, Iran.

Her research activity is mainly focus on polarimetric SAR images, change detection techniques, and Object-based image analysis.

Mahmod Reza Sahebi received the B.Sc. degree in civil engineering from the Amirkabir University of Technology, Tehran, Iran, in 1991, the M.Sc. degree in civil engineering in 1996, and the Ph.D. degree in remote sensing in 2003 from the University de Sherbrooke, Sherbrooke, QC, Canada.

From 2003 to 2006, he worked as a Postdoctoral Fellow in the Canadian Space Agency. He is currently an Associate Professor and the Head of remote sensing research center in the Department of Geodesy and Geomatics engineering, K.N Toosi University of Technology, Tehran, Iran.